AIP | Applied Physics Letters

Tip-enhanced fluorescence microscopy of high-density samples

Changan Xie, Chun Mu, Jonathan R. Cox, and Jordan M. Gerton

Citation: Applied Physics Letters **89**, 143117 (2006); doi: 10.1063/1.2358122
View online: http://dx.doi.org/10.1063/1.2358122
View Table of Contents: http://scitation.aip.org/content/aip/journal/apl/89/14?ver=pdfcov
Published by the AIP Publishing

Tip-enhanced fluorescence microscopy of high-density samples

Changan Xie, Chun Mu, Jonathan R. Cox, and Jordan M. Gerton[a)]
Physics Department, University of Utah, 115 S. 1400 E., Rm. 201, Salt Lake City, Utah 84112

(Received 23 June 2006; accepted 11 August 2006; published online 6 October 2006)

High-density samples of fluorescent quantum dots (QDs) were imaged using an apertureless near-field optical microscopy technique. QD fluorescence was modulated by oscillating a silicon atomic force microscope tip above an illuminated sample and a lock-in amplifier was used to suppress background from the excitation laser. Spatial resolution near 10 nm and a peak signal-to-noise ratio (SNR) of ~60 were achieved. Individual QDs within high-density ensembles were still easily resolved (SNR>5) at a density of 14 QDs/μm^2. These results have favorable implications for the eventual nanoscale imaging of viable biological systems, such as cellular membranes. © *2006 American Institute of Physics*. [DOI: 10.1063/1.2358122]

Various efforts in optical microscopy have been devoted to overcome the resolution limit imposed by classical light diffraction. Near-field scanning optical microscopy (NSOM) is one technique that breaks the diffraction barrier by forcing light through a nanoscale aperture in close proximity to a surface.[1,2] Although 30 nm resolution is theoretically possible, resolution below 50 nm is seldom seen due to the severe cutoff in light transmission efficiency for small apertures. Apertureless NSOM (ANSOM) circumvents this limit by replacing the small aperture with a sharp tip in the focus of a laser beam. The nano-optical field in the vicinity of the tip apex is strongly enhanced due to either the resonant excitation of localized surface plasmons[3] or a geometric lightning-rod effect.[4]

One of the most intriguing potential applications of ANSOM is for imaging viable biological samples *in vitro*. Other high-resolution techniques such as electron microscopy and x-ray crystallography can yield structural information with exquisite detail, but are not compatible with physiological conditions. For biological imaging, ANSOM should be sensitive to individual molecules within high-density ensembles. Unfortunately, multiple molecules within the excitation-laser focus raise the background and lower the signal-to-noise ratio (SNR). Thus for biological applications, it is essential to optimize the factors that influence ANSOM contrast.

Fluorescence spectroscopy is the most straightforward way to achieve single-molecule sensitivity in ANSOM because of the large absorption cross sections and because it is essentially free of topographical artifacts.[5] Several previous demonstrations of ANSOM with both one- and two-photon fluorescence have been reported.[6–13] Here, we studied the contrast of an ANSOM technique, called tip-enhanced fluorescence microscopy (TEFM), which combines tapping-mode atomic force microscopy (AFM) with confocal fluorescence microscopy (Fig. 1). The enhanced intensity distribution is tightly confined near the tip apex, so oscillating the AFM probe modulates the fluorescence signal. We used a lock-in amplifier for demodulation and studied the dependence of the SNR on tapping amplitude for isolated semiconductor nanocrystal quantum dots (QDs). Further, we studied the SNR of single QDs within high-density ensembles and observed good SNR for densities up to ~15 QDs/μm^2.

A simplified schematic of the experiment is shown in Fig. 1. An AFM (Asylum MFP-3D) was mounted above an inverted microscope (Nikon TE 2000-U). A green He–Ne laser beam (λ=543 nm) was focused onto a glass coverslip through a high numerical-aperture objective (NA=1.4, 100 ×). A 60° crescent mask was inserted before the objective to achieve evanescent illumination within a nearly diffraction-limited focal spot (0.5×1.0 μm^2). The polarization of the laser beam was adjusted to give a strong axial component at the surface as required for lightning-rod enhancement.[4,14] Silicon tips were used since they do not induce fluorescence quenching, in contrast to metallic probes.[8,11] The AFM tip was aligned into the center of the illumination spot, and the emitted QD fluorescence was collected by the objective, spectrally filtered (Chroma HQ605/75), and focused onto an avalanche photodiode (Perkin-Elmer SPCM-AQR-13).

Voltage pulses corresponding to individual photocounts were input directly to a commercial lock-in amplifier (SRS SR830). The digital signal used to drive the tip oscillation (~70 kHz frequency) was used as the lock-in reference.[15] The amplitude portion of the lock-in signal was low-pass filtered with a time constant corresponding to the AFM pixelation and was acquired as the TEFM image along with the topography and total photon-sum images.

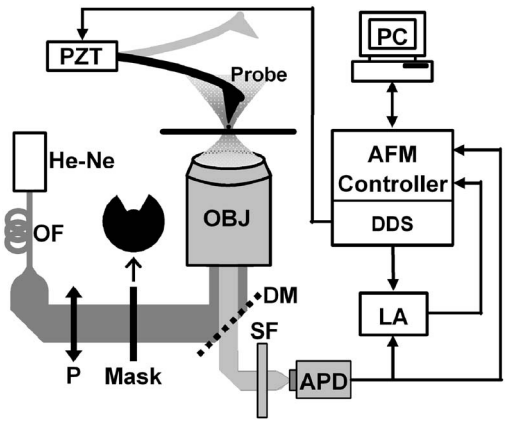

FIG. 1. Simplified schematic diagram of the experiment. APD: avalanche photodiode; DDS: direct digital synthesizer; DM: dichroic mirror; SF: spectral filter; LA: lock-in amplifier; OBJ: objective; PC: personal computer; P: polarizer; PZT: piezoelectric transducer; OF: optical fiber.

[a)]Author to whom correspondence should be addressed; electronic mail: jgerton@physics.utah.edu

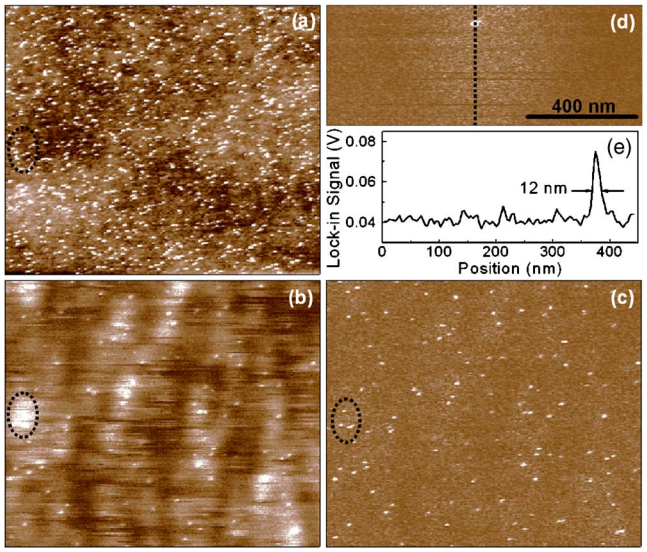

FIG. 2. (Color online) High-resolution images of quantum dots. (a) AFM image (topography); (b) photon-sum image; (c) TEFM image. (a)–(c) are for a 5×5 μm^2 field of view. (d) TEFM image of a single quantum dot; (e) signal profile specified by the dotted line in (d).

Figures 2(a)–2(c) show the topography, photon-sum, and TEFM images, respectively, for a 5×5 μm^2 field of view. The three images were acquired simultaneously using an ATEC-FM-10 probe (Nanosensors). Samples were prepared by drying a diluted sample of CdSe–ZnS core-shell quantum dots (Invitrogen Q21701MP) onto a clean glass coverslip. The average QD diameter is ~4 nm and the emission maximum (as per specifications) is at $\lambda=606$ nm. A typical far-field count rate of $\sim4\times10^4$ s^{-1} was observed for an excitation power of ~160 nW. The fluorescence rate from single QDs is highly dynamic, exhibiting "blinking" and sudden changes in quantum yield, in agreement with previous observations.[16] Although only ~20% of the QDs were optically active, there was always a 1:1 correlation between the far-field and near-field fluorescence signals for isolated QDs.

The TEFM contrast is clearly superior to that of the photon sum. For example, it is difficult to judge how many active QDs there are in the photon-sum image within the area encircled by the dashed lines due to the high far-field background. The TEFM image shows four distinct QDs, two of which (lower right) are ~60 nm apart. Figure 2(d) shows the TEFM image of a single isolated QD and Fig. 2(e) shows the signal profile along the indicated axis. The full width at half maximum is about 12 nm, which is close to the radius of curvature of the probe apex as determined from the height trace (data not shown). The width of the signal profile suggests a spatial resolution near 10 nm, limited only by the probe sharpness.[12] Note that a horizontal profile (along the fast-scan axis) gives a width of ~19 nm. This difference is not due to artifacts arising from image reconstruction; rather it arises from a slight eccentricity in the QD shape convolved with the shape of the tip.

In tapping-mode AFM, the optical contrast of both the photon-sum and TEFM images is effected by the probe oscillation amplitude. Figure 3 depicts the SNR of TEFM (photon-sum) images versus peak-peak probe amplitude for isolated QDs (density much less than one QD per illumination-spot area). The SNR for each QD image was computed according to the following:

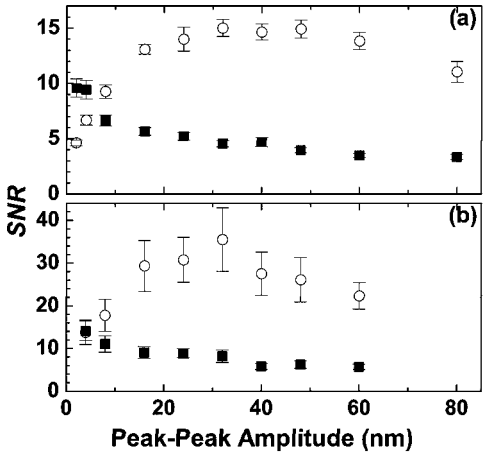

FIG. 3. Optimization of oscillation amplitude. (a) BudgetSensors Multi75 probes; (b) Nanosensors ATEC-FM-10 probes. Open circles: TEFM data; solid squares: photon-sum data. A total of 9 QDs was measured in (a) and 12 in (b) using two to three different tips for each data set. Each data point is the mean of all QDs measured and error bars are the standard error. The uncertainty in the oscillation amplitude is ~10%.

$$\mathrm{SNR}=\frac{\langle s_{\mathrm{peak}}\rangle-\langle s_{\mathrm{bg}}\rangle}{\sigma_{\mathrm{bg}}}, \tag{1}$$

where s_{peak} is the peak lock-in (photon-sum) signal at the QD location, s_{bg} is the lock-in (photon-sum) signal corresponding to the background, and σ_{bg} is the standard deviation of the background lock-in (photon-sum) signal. To suppress fluctuations, s_{peak} is averaged over a few pixels at the center of the QD, s_{bg} is averaged over a thin annulus surrounding the QD, and σ_{bg} is computed from the same annulus.

The enhanced field has very short range, decaying within 5–10 nm of the tip apex for the sharpest probes.[12] Thus for large amplitudes, the QD experiences only moderate enhancement in the excitation rate, *on average*, as the tip spends only a small fraction of its oscillation cycle close to the sample surface. In this case, both the photon-sum and TEFM images exhibit relatively low contrast. For amplitudes smaller than the enhancement decay length, the fluorescence rate is never fully modulated resulting in a loss of contrast for the TEFM image. Further, at the smallest amplitudes (<4 nm) the AFM may enter "attractive" or "noncontact" operation mode, in which case the tip maintains a minimum separation (1–3 nm) from the sample at closest approach, resulting in further loss of contrast. On the other hand, small amplitudes lead to favorable contrast for the photon-sum image since the tip spends its entire oscillation cycle within an enhancement decay length of the sample surface.

The data shown in Fig. 3(a) were obtained using BudgetSensors probes (Multi75). The broad peak in the TEFM data between about 25 and 60 nm amplitudes results from the competition between incomplete modulation at small amplitudes and reduced average enhancement at large amplitudes. Figure 3(b) shows the data collected with Nanosensors probes (ATEC-FM-10); the general trends in the data are similar to the Multi75 probes, although the peak in SNR for the TEFM data is higher, narrower, and shifted to slightly smaller amplitudes. The ATEC tips were somewhat sharper on average, leading to better performance (see below).

One might expect that optimum contrast would occur for amplitudes roughly equivalent to the enhancement decay length, or about 10–15 nm in our case. This is clearly incon-

sistent with the measurements. One explanation for this disagreement is that the data in Fig. 3 are composed of an average of many measurements on different QDs using several different tips with varying sharpness. This tends to broaden the peak somewhat, particularly toward larger amplitudes, since the tip sharpness determines the enhancement decay length,[12] which in turn affects the optimum amplitude. Another possibility is that phase noise in the probe's oscillatory motion decreases the lock-in signal because the phase corresponding to tip-sample contact becomes less well defined. These possibilities are currently being investigated experimentally and with Monte Carlo simulations.

The larger SNR for the ATEC probes may be due to the fact that they are sharper (7–10 nm radius of curvature versus 12–15 nm for the Multi75 tips), leading to larger field enhancement.[3,4] In addition, enhancement strength is very sensitive to the relative angle between the tip axis and the local polarization direction (approximately vertical) as well as the geometric symmetry of the tetrahedral probes. When mounted on the AFM head, the ATEC tip axis is more vertical than the Multi75, which should lead to greater coupling to the laser illumination and thus larger enhancement strength.[14] Further, the average half-cone angle at the tip apex is $<5°$ for the ATEC probes and is $\sim 10°$ for the Multi75 probes according to their specifications. This should also give the ATEC probes an advantage in enhancement strength.[17] Finally, differences in bulk-dopant concentration and uncontrolled surface properties (i.e., contaminants and oxide layers) can cause variations in the enhancement strength between the two types of probes.

We note that the variation in SNR among the data corresponding to ATEC probes is significantly larger than for the Multi75 probes, leading to larger error bars in Fig. 3(b). For 6 out of the 12 QDs in this data set, we measured an average SNR that peaked at ~ 60 while the other 6 gave SNRs moderately higher than the Multi75 measurements. We believe this variation may be due to graininess in the raster images. To facilitate data acquisition speed, we chose to acquire 1 μm^2 images broken into 256×256 pixels. Thus the size of each pixel (4×4 nm^2) is roughly equivalent to the lateral size of a single QD. Since the size of the ATEC tip is only about double this (see above), the tip apex will often skirt the center of the QD, resulting in smaller fluorescence enhancement. The Multi75 tips are much larger than the ATECs, giving more consistent, albeit lower, contrast.

Our measurements of high-density samples consisted of dozens of 1×1 μm^2 images of multiple QDs. Due to the large volume of data, it was impractical to reduce the pixel size for these measurements to alleviate the variations in SNR described above for ATEC tips. Thus we chose Multi75 tips for their consistent contrast and accept that improved SNR can be achieved for any given image by using ATEC tips. When multiple QDs are illuminated simultaneously, the lock-in signal becomes noisier at every tip location. Thus, as the QD density increases, a concomitant reduction in SNR is observed, as shown in Fig. 4. These data were collected by preparing QD samples with different dilution factors, and then randomly scanning 1×1 μm^2 frames. Each image was categorized according to its active QD density, as determined by TEFM, and individual QDs within the frame were analyzed as above. This was repeated for many different frames and several different tips were used to complete the measurement. The experiment shows that TEFM enables high-fidelity imaging even for the largest densities measured.

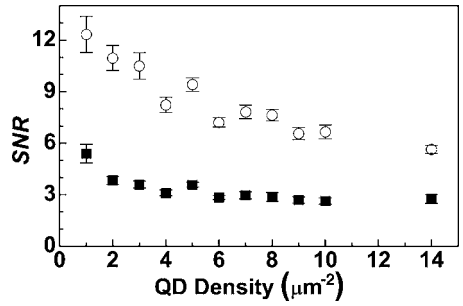

FIG. 4. Image contrast at high density. Open circles: TEFM data; solid squares: photon-sum data. Each data point is the mean of at least ten different quantum dots and error bars are the standard error.

In conclusion, this work demonstrated unambiguously that TEFM is well suited for imaging high-density samples of fluorescent particles with nanoscale resolution. The highest densities imaged here are comparable to many fluorescently labeled biological systems. To achieve the sensitivity needed to interrogate these systems, it is critical to optimize various parameters including the tip-oscillation amplitude, the method of data acquisition (e.g., lock in versus photon sum), and the physical parameters of the tip. In the future, we will implement time-tagged photon counting,[12,18] which enables complete flexibility in the data analysis and possibly large improvements in the SNR. Further, we will extend this technique to liquid imaging for application to *in vitro* biological systems such as lipid membranes.

[1] D. W. Pohl, W. Denk, and M. Lanz, Appl. Phys. Lett. **44**, 651 (1984).
[2] A. Harootunian, E. Betzig, M. S. Isaacson, and A. Lewis, Appl. Phys. Lett. **49**, 674 (1986).
[3] Y. C. Martin, H. F. Hamann, and H. K. Wickramasinghe, J. Appl. Phys. **89**, 5774 (2001).
[4] L. Novotny, R. X. Bian, and X. S. Xie, Phys. Rev. Lett. **79**, 645 (1997).
[5] B. Hecht, H. Bielefeld, Y. Inouye, D. W. Pohl, and L. Novotny, J. Appl. Phys. **81**, 2492 (1997).
[6] E. J. Sanchez, L. Novotny, G. R. Holtom, and X. S. Xie, J. Phys. Chem. A **101**, 7019 (1997).
[7] E. J. Sanchez, L. Novotny, and X. S. Xie, Phys. Rev. Lett. **82**, 4014 (1999).
[8] T. J. Yang, G. A. Lessard, and S. R. Quake, Appl. Phys. Lett. **76**, 378 (2000).
[9] H. F. Hamann, M. Kuno, A. Gallagher, and D. J. Nesbitt, J. Chem. Phys. **114**, 8596 (2001).
[10] V. V. Protasenko, M. Kuno, A. Gallagher, and D. J. Nesbitt, Opt. Commun. **210**, 11 (2002).
[11] W. Trabesinger, A. Kramer, M. Kreiter, B. Hecht, and U. P. Wild, Appl. Phys. Lett. **81**, 2118 (2002).
[12] J. M. Gerton, L. A. Wade, G. A. Lessard, Z. Ma, and S. R. Quake, Phys. Rev. Lett. **93**, 180801 (2004).
[13] H. G. Frey, S. Witt, K. Felderer, and R. Guckenberger, Phys. Rev. Lett. **93**, 200801 (2004).
[14] L. Aigouy, A. Lahrech, S. Gresillon, H. Cory, A. C. Boccara, and J. C. Rivoal, Opt. Lett. **24**, 187 (1999).
[15] Using the actual tip-oscillation signal as the lock-in reference made no appreciable difference for this work.
[16] R. G. Neuhauser, K. T. Shimizu, W. K. Woo, S. A. Empedocles, and M. G. Bawendi, Phys. Rev. Lett. **85**, 3301 (2000).
[17] J. L. Bohn, D. J. Nesbitt, and A. Gallagher, J. Opt. Soc. Am. A **18**, 2998 (2001).
[18] Y. Ebenstein, E. Yoskovitz, R. Costi, A. Aharoni, and U. Banin, J. Phys. Chem. A **110**, 8297 (2006).